

# Chemiluminescent Labels Released from Long Spacer Arm-Functionalized Magnetic Particles: A Novel Strategy for Ultrasensitive and Highly Selective Detection of Pathogen Infections

Haowen Yang,<sup>†</sup> Wenbiao Liang,<sup>‡</sup> Nongyue He,<sup>\*,†</sup> Yan Deng,<sup>†</sup> and Zhiyang Li<sup>\*,§</sup>

<sup>†</sup>State Key Laboratory of Bioelectronics, School of Biological Science and Medical Engineering, Southeast University, Nanjing 210096, China

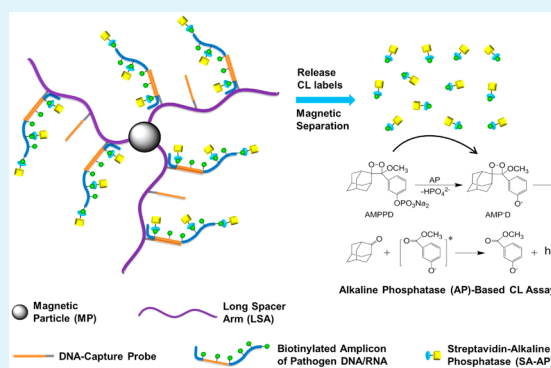
<sup>‡</sup>Jiangsu Province Blood Center, Nanjing 210042, China

<sup>§</sup>Department of Laboratory Medicine, Second Affiliated Hospital of Nanjing Medical University, Nanjing 210011, China

## Supporting Information

**ABSTRACT:** Previously, the unique advantages provided by chemiluminescence (CL) and magnetic particles (MPs) have resulted in the development of many useful nucleic acid detection methods. CL is highly sensitive, but when applied to MPs, its intensity is limited by the inner filter-like effect arising from excess dark MPs. Herein, we describe a modified strategy whereby CL labels are released from MPs to eliminate this negative effect. This approach relies on (1) the magnetic capture of target molecules on long spacer arm-functionalized magnetic particles (LSA-MPs), (2) the conjugation of streptavidin-alkaline phosphatase (SA-AP) to biotinylated amplicons of target pathogens, (3) the release of CL labels (specifically, AP tags), and (4) the detection of the released labels. CL labels were released from LSA-MPs through LSA ultrasonication or DNA enzymolysis, which proved to be the superior method. In contrast to conventional MPs, LSA-MPs exhibited significantly improved CL detection, because of the introduction of LSA, which was made of water-soluble carboxymethylated  $\beta$ -1,3-glucan. Detection of hepatitis B virus with this technique revealed a low detection limit of 50 fM, high selectivity, and excellent reproducibility. Thus, this approach may hold great potential for early stage clinical diagnosis of infectious diseases.

**KEYWORDS:** chemiluminescent label, magnetic particle, long spacer arm, ultrasensitive detection, infectious pathogen



## INTRODUCTION

Over the past several decades, significant efforts have been devoted to the development of strategies for nucleic acid detection in biological and biomedical applications, such as genome or gene expression analysis,<sup>1,2</sup> polymorphism or mutation detection,<sup>3,4</sup> DNA sequencing,<sup>5,6</sup> and the diagnosis of infectious or genetic diseases.<sup>7–9</sup> Nucleic acid hybridization-based detection methods typically involve the hybridization of immobilized DNA-capture probes to target DNA, which is usually detected via label-based strategies. In recent years, a variety of label-based DNA detection assays have been developed using optical or electrochemical techniques to amplify the detection signals. Many electrochemical techniques involving redox molecules,<sup>10</sup> carbon nanotubes,<sup>11,12</sup> and silicon nanowires<sup>13</sup> are novel and successful but lack practicality for clinical applications. Notably, optical techniques may or may not require the use of a label, and label-free methodologies, such as surface plasmon resonance,<sup>14</sup> surface-enhanced Raman scattering,<sup>15</sup> atomic force microscopy,<sup>16</sup> and piezoelectric sensors,<sup>17</sup> have all attracted significant attention. However, the sensitivities of these methods are not comparable to those of label-based methods, and these methods require expensive

instrumentation. Thus, optical labels, including fluorescent tags,<sup>18,19</sup> chemiluminescent (CL) labels,<sup>20,21</sup> and colorimetric nanoparticles,<sup>22–24</sup> are typically used for clinical DNA detection. Among these, fluorescence- and CL-based strategies are the most practical and extensively exploited approaches in clinical analysis. Notably, in contrast to fluorescence, CL has an ultralow background and greater sensitivity; thus, CL detection is superior to fluorescence-based detection because of its high sensitivity, wide calibration range, and simple instrumentation. CL assays for DNA detection are commonly performed using capillary electrophoresis,<sup>25</sup> microfluidic sensors,<sup>26</sup> magnetic particles,<sup>27–29</sup> and paper-based nanobiosensors.<sup>30</sup>

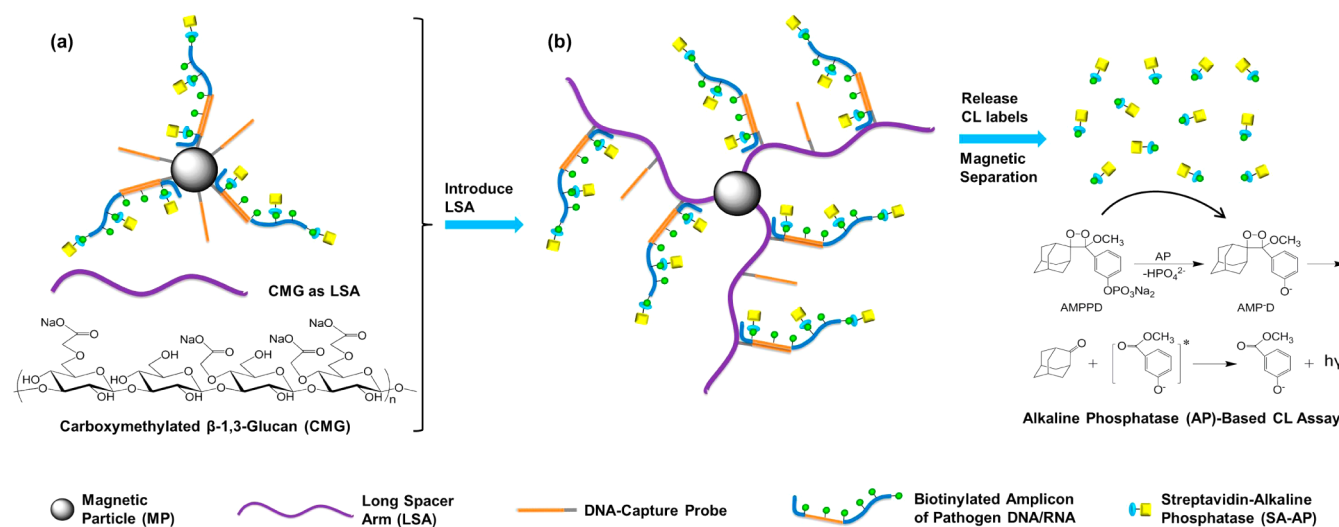
In a typical hybridization-based nucleic acid detection scheme, it is crucial to develop a highly effective hybridization strategy to improve the detection of nucleic acids at low levels in real samples. In recent years, the rapid development of nanotechnology has allowed nucleic acid hybridization on nanomaterials such as magnetic particles (MPs). MPs have

Received: October 17, 2014

Accepted: December 18, 2014

Published: December 31, 2014

**Scheme 1. Diagram of Enhanced Chemiluminescent (CL) Detection of a Target Pathogen Based on Released CL Labels from Long Spacer Arm-Functionalized Magnetic Particles (LSA-MPs)<sup>a</sup>**



<sup>a</sup>Genomic DNA/RNA of a target pathogen is isolated from patient serum samples, and biotinylated amplicons are produced by polymerase chain reaction (PCR) or reverse transcription PCR (RT-PCR) using biotin-11-dUTP. Subsequently, the biotinylated amplicons are captured by LSA-MPs and then conjugated with streptavidin-alkaline phosphatase (SA-AP). After treatment with deoxyribonuclease (DNase) or ultrasonic vibration and magnetic separation, the released CL labels (namely, AP tags) catalytically convert the substrate AMPPD to AMP<sup>+</sup>D, and the phenoxide intermediate immediately decomposes with the emission of a strong, prolonged CL signal. (a) MP-based CL detection method. (b) Carboxymethylated  $\beta$ -1,3-glucan (CMG) as LSA, forming LSA-MPs for enhanced CL detection.

considerable advantages in the detection of nucleic acid because of their unique features, including excellent biocompatibility, rapid magnetic separation, and large surface area-to-volume ratios for nucleic acid conjugation.<sup>31,32</sup> Because CL labels and MPs have unique chemical properties, our group recently described the development of an Fe<sub>3</sub>O<sub>4</sub>@SiO<sub>2</sub> MP-based CL approach for the detection of sequence-specific DNA found in infectious pathogens, using the CL system of alkaline phosphatase (AP) and 3-(2'-spiroadamantyl)-4-methoxy-4-(3''-phosphoryloxy)phenyl-1,2-dioxetane (AMPPD) (a in Scheme 1).<sup>33–35</sup> In spite of its elegance, the limited detection sensitivity caused by steric hindrance resulting from DNA hybridization remains to be improved. To solve this problem, we employed water-soluble carboxymethylated  $\beta$ -1,3-glucan (CMG) as a long spacer arm (LSA) conjugated with aminated DNA-capture probes on MPs (b in Scheme 1).<sup>36</sup> In contrast to conventional MPs,<sup>28,33–35</sup> the long spacer arm-functionalized magnetic particles (LSA-MPs) have significant advantages in terms of DNA hybridization as a direct consequence of their long and flexible spacer arms, which give almost full freedom for DNA hybridization near the MP surface. Importantly, compared with other modified MP-based detection methods,<sup>37,38</sup> this novel strategy for the conjugation of LSA is simple, convenient, and cost-effective because the spacer molecules do not require functionalization.

In previous studies, we found that CL intensities were significantly attenuated by MPs and sharply declined with increasing levels of MPs (Figure S1, Supporting Information). This phenomenon tremendously limited the high-sensitivity performance of CL labels applied to MPs, and it was presumably caused by an inner filter-like effect from excess dark MPs.<sup>39</sup> To resolve this problem, CL labels should be released from MPs such that the target can be independently detected and the attenuation in CL intensity can be prevented. To accomplish this in our strategy, the LSA-containing capture

probes are linked to MPs through covalent attachment and then hybridize with target DNA fragments modified with CL labels, as shown in Scheme 1. Therefore, upon DNA degradation or LSA fracture, it is anticipated that CL labels can be released from the LSA-MPs. In this study, we employed two methods for the release of CL labels, one involving DNA enzymolysis and another involving LSA ultrasonication. These strategies could be integrated into our previous CL detection technique as an important improvement significantly enhancing detection sensitivity. The modified approach relies on the magnetic capture of target molecules by LSA-MPs, conjugation of streptavidin-alkaline phosphatase (SA-AP) to biotinylated amplicons of the target pathogen, release of CL labels (namely, AP tags), and the detection of released tags (Scheme 1). The released CL labels were detected upon mixing with AMPPD, as the mixture generated a prolonged CL signal in response to catalysis by the AP tags conjugated to the target DNA.<sup>20,21</sup> Unlike previous MP-based methods that suffer from attenuated CL intensities, the strategy herein reported completely avoids this negative effect. We anticipate that this novel method will significantly improve the sensitivity of MP-based CL approaches for the ultrasensitive detection of target pathogens in clinical samples, demonstrating that our method has great promise for the early stage diagnosis of pathogenic infections.

## EXPERIMENTAL SECTION

**Materials and Instruments.** Aminated MPs (~400 nm in diameter) and CMG (700 kDa) were provided by Nanjing Longliang Biological Science and Technology Co., Ltd. (3-Aminopropyl)-triethoxysilane (APTES) and the hybridization solution were purchased from Sigma-Aldrich. PCR reagents, dATP, dCTP, dGTP, dTTP, 1-ethyl-3-[3-(dimethylamino)propyl]carbodiimide hydrochloride (EDC-HCl), and SA-AP were purchased from Sangon Biotech (Shanghai) Co., Ltd. The TIANamp Virus DNA/RNA Kit was purchased from TIANGEN Biotech (Beijing) Co., Ltd. Biotin-11-dUTP was purchased from Thermo Fisher Scientific Inc. AMPPD was

purchased from Sichuan Biochem-ZX Research Co., Ltd. The AxyPrep DNA Gel Purification Kit was purchased from Axygen Scientific Inc. MES buffer (pH 6) was prepared by dissolving 2-morpholinoethanesulfonic acid monohydrate (MES) in deionized water. Wash buffer (pH 7.4) was prepared by dissolving Tris and NaCl in deionized water. Microtiter plates (96-well) were purchased from Greiner. Serum samples from patients infected with hepatitis B virus (HBV), hepatitis C virus (HCV), human immunodeficiency virus (HIV), and *Treponema pallidum* (TP) and from healthy subjects had been qualitatively screened by the Roche COBAS AmpliPrep/COBAS TaqMan System and were provided by Jiangsu Province Blood Center. PCR was performed with an ABI9700 Thermocycler (Applied Biosystems). CL intensity was detected by a 2030 Multilabel Plate Reader (PerkinElmer).

**Experimental Procedures. Primer and Probe Design.** HBV, an infectious pathogen, was selected to assess the feasibility of this approach. The primers and probe were designed using Premier Primer 5 software (PREMIER Biosoft) (Table S1, Supporting Information) and synthesized by Sangon Biotech. The target amplicon sequence was located in a conserved domain of the HBV gene sequence, and the probe was completely complementary to the antisense strand of the target amplicon.

**Preparation of LSA-MPs.** LSA-MPs, specifically CMG-MPs, were prepared by the conjugation of CMG and aminated MPs.<sup>36</sup> Briefly, 6  $\mu\text{L}$  of APTES was added to a solution of 3 mL of ethanol mixed with 15 mg of  $\text{Fe}_3\text{O}_4@ \text{SiO}_2$  and stirred for 7 h at 25  $^\circ\text{C}$  to obtain aminated MPs. Aminated MPs (1 mL, 10 mg/mL) were added to 1 mL of a 5 mg/mL CMG solution (dissolved in MES buffer), and EDC·HCl (3 mg/mL) was used as an activating agent. After overnight incubation at 4  $^\circ\text{C}$ , the conjugates were washed twice with MES buffer. The final concentration of CMG-MPs was 5 mg/mL.

**Probe Immobilization on LSA-MPs.** Probes were attached to CMG-MP surfaces by covalent binding. CMG-MPs (1 mg) were incubated with 100  $\mu\text{L}$  of a 5  $\mu\text{M}$  aminated DNA probe solution and diluted with MES buffer for 7 h with the addition of EDC·HCl (10 mg/mL). Next, the probe-modified CMG-MPs (MP-CMG-probes) were washed several times and dispersed in 100  $\mu\text{L}$  of PBS buffer (0.1 M, pH 7.4).

**Preparation of the Biotinylated Amplicon.** Genomic DNA (HBV, TP, control 1) and total RNA (HCV, control 2; HIV, control 3) were extracted from patient serum samples using the TIANamp Virus DNA/RNA Kit according to the manufacturer's protocol. Subsequently, the HBV and TP biotinylated amplicons were prepared by PCR with the genomic DNA template, 0.25  $\mu\text{M}$  primers, and PCR mixtures. The biotinylated HCV and HIV amplicons were prepared by RT-PCR with the total RNA template, 5 units of AMV reverse transcriptase, 5 units of RNasin, and PCR mixtures. PCR mixtures contained 1 $\times$  Taq buffer, 1.5 mM  $\text{MgCl}_2$ , 0.25 mM dATP, 0.25 mM dGTP, 0.25 mM dCTP, 0.21 mM dTTP, 0.04 mM biotin-11-dUTP, and 5 units of Taq DNA polymerase in 50  $\mu\text{L}$ . The PCR process consisted of a 5 min initial melting step at 95  $^\circ\text{C}$ , followed by 35 cycles of 30 s at 95  $^\circ\text{C}$ , 30 s at 58  $^\circ\text{C}$ , and 45 s at 72  $^\circ\text{C}$ , and a final extension step of 7 min at 72  $^\circ\text{C}$ . The PCR products were purified with the AxyPrep DNA Gel Purification Kit. The molecular weights of the amplicons were confirmed by agarose gel electrophoresis, and the concentrations were determined by measuring the absorbance at 260 nm with a UV-vis spectrophotometer.<sup>40</sup>

**Hybridization Reaction and SA-AP Incubation.** The biotinylated amplicons were collected with MP-CMG-probes through a hybridization reaction. MP-CMG-probes (30  $\mu\text{L}$ , 5 mg/mL) were added to a PCR tube, and the supernatant was discarded after magnetic separation.<sup>33–35</sup> A mixture containing 10  $\mu\text{L}$  of hybridization solution, 9  $\mu\text{L}$  of deionized water, and 1  $\mu\text{L}$  of biotinylated amplicon was added to the PCR tube and the tube heated to 95  $^\circ\text{C}$  for 3 min, followed by hybridization at 60  $^\circ\text{C}$  for 10 min. The hybridized products were successively cleaned by being washed with 2 $\times$  sodium citrate (SSC) buffer, 0.1 $\times$  SSC buffer, and wash buffer. The hybridized products were incubated with SA-AP for 30 min. Subsequently, the complexes were cleaned again by being washed several times with wash buffer.

**CL Detection of Released Labels.** To release the CL labels from the LSA-MPs, two methods were carried out.

**DNase I Treatment.** The cleaned magnetic complexes were resuspended in 50  $\mu\text{L}$  of PBS buffer (pH 7.4); 50  $\mu\text{L}$  of a DNase I solution (15 units) was added, and the mixture was incubated for 10 min.

**Ultrasonic Treatment.** The cleaned, magnetic complexes were resuspended in 100  $\mu\text{L}$  of PBS buffer (pH 7.4) and treated with ultrasonic vibration at 40 kHz (100 W) for 30 min. After treatment with one of the two strategies, the supernatant was collected and transferred to a new tube after magnetic separation for 5 min. Upon addition of 100  $\mu\text{L}$  of 0.25 mM AMPPD, CL intensities were recorded by a 2030 Multilabel Plate Reader every 5 min for 60 min. Meanwhile, the remaining magnetic complexes were washed, and CL detection was performed following the same steps.

## RESULTS AND DISCUSSION

CMGs were conjugated on the surface of aminated MPs by amino/carboxyl interaction. To confirm this CMG modification, several characterization experiments were performed. The morphology and particle size of MPs was observed by transmission electron microscopy (TEM) and scanning electron microscopy (SEM), but no obvious distinction was found between the samples before and after CMG modification. (Figure S2A, Supporting Information). The size determined by dynamic light scattering (DLS) showed that the average hydrodynamic size of MPs increased from 677.9 to 772.2 nm in CMG-MPs (Figure S2B, Supporting Information). Meanwhile, the  $\zeta$  potential measured by DLS changed upon surface modification from 14.3 mV for aminated MPs to  $-12.4$  mV for CMG-MPs. The increase in size and the positive-negative change in  $\zeta$  potential were attributed to the negatively charged CMG on the MP surface. These observations provided evidence of the successful conjugation of CMG onto MPs.

Scheme 1 presents a schematic diagram of the enhanced CL detection of target pathogens based on CL labels released from LSA-MPs. In the presence of a target pathogen, the biotinylated amplicons prepared by PCR and/or RT-PCR are conjugated with SA-AP, and the substrate, AMPPD, is catalytically dephosphorylated. Subsequently, the phenoxide intermediate immediately decomposes and emits a strong, prolonged CL signal.<sup>21</sup> In this study, DNase I was used to degrade DNA to release the labels, because DNase I nonspecifically degrades single- or double-stranded DNA to mononucleotides or oligonucleotides.<sup>41</sup> As a proof of principle, HBV was utilized as a model system to demonstrate the potential diagnostic significance of this technique. As expected, typical CL dynamic curves were obtained upon detection of HBV-positive samples, while only an insignificant CL signal was observed in the negative control, because of the inability to form biotinylated amplicons in the absence of HBV. As shown in Figure 1A, the detection of released CL labels contributed to a 10-fold increase in CL intensities, in contrast to MP-retained CL detection. Notably, after releasing the CL labels, the remaining LSA-MPs still emitted a significantly strong signal compared with that of the negative control (c in Figure 1A), indicating that the DNA adjacent to the MP surface could not be fully degraded as a result of the retention of a few CL labels. In addition, gel electrophoresis analysis, which presented clear bands with a size of 126 bp, validated the successful formation of the biotinylated HBV amplicons and the lack of formation of nontarget amplicons (Figure S3, Supporting Information). To further verify detection specificity, HCV, HIV, and TP were detected as controls. As shown in Figure 1B, only HBV detection yielded a

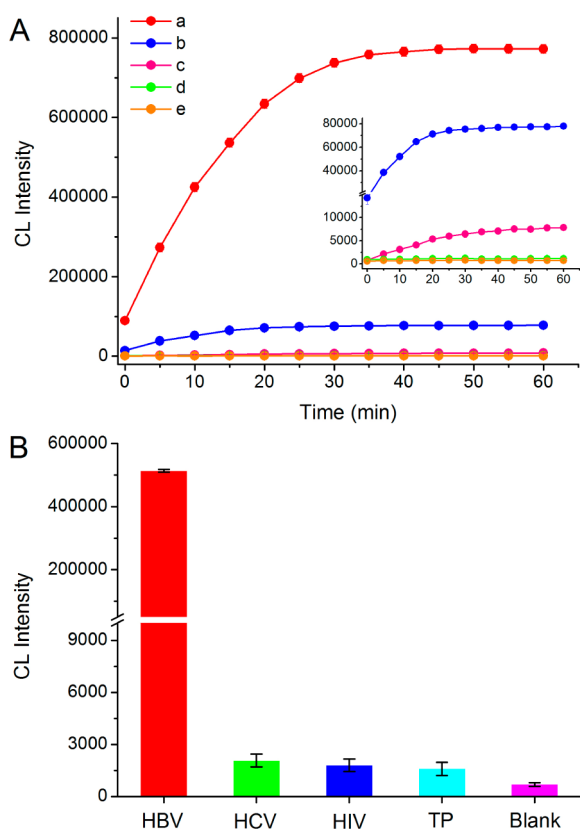


**Figure 1.** (A) CL dynamic curves representing CL detection of HBV amplicons based on LSA-MPs. CL detection of the released CL labels (a), LSA-MPs conjugated with CL labels (b), LSA-MPs remaining after CL labels are released (c), negative-strand HBV DNA (d), and deionized water (e). The CL intensities for each sample were recorded every 5 min by a PerkinElmer 2030 Multilabel Plate Reader. (B) Specificity test of the developed detection technique. HBV, HCV, HIV, and TP were detected. Deionized water was detected as a blank control. Error bars show the standard deviations of three independent measurements.

strong CL intensity, demonstrating the high specificity of this technique.

As a noninvasive method for releasing CL labels and in an attempt to simplify the procedure, another strategy was employed to release CL labels, namely ultrasonic vibration. In this method, CL labels (AP tags) were released through the ultrasonic degradation of the CMG LSAs, which were degraded according to the midpoint scission of polymers by ultrasound-induced mechanical effects.<sup>42</sup> In the pre-experiment, ultrasonic vibration was executed at 40 kHz (100 W) for 10 min. However, only a few CL labels were released under these conditions. Thus, we investigated the release efficiency of CL labels at frequencies of 40, 120, and 500 kHz (100 W) by monitoring changes in CL intensity. After ultrasonication at 500 kHz, the CL intensity was higher than that with ultrasonication at 40 and 120 kHz (Figure 2); however, the CL intensity was still much lower than that observed with the DNase I treatment. Moreover, the CL intensity after ultrasonication at 500 kHz remained virtually constant between 10 and 30 min, and the intensity merely doubled that of the remaining LSA-MPs, indicating that ultrasonication was not as efficient as DNase degradation. Therefore, we utilized DNase degradation for the release of CL labels in the subsequent assays.

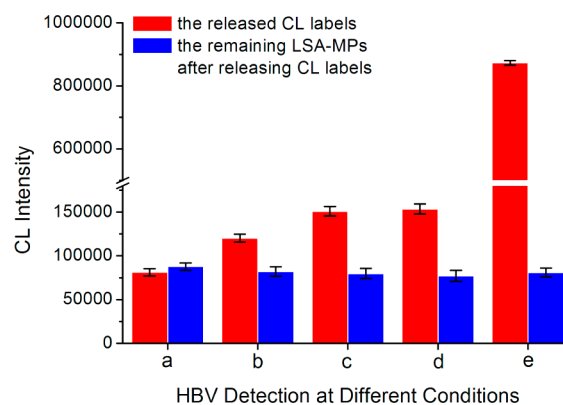


**Figure 2.** CL detection of HBV at ultrasonic frequencies of (a) 40, (b) 120, and (c) 500 kHz for 10 min and (d) 500 kHz for a 30 min ultrasonic vibration. (e) DNase I degradation-based CL detection of HBV was used as a control. The detection procedure was performed as described in the Experimental Section. Error bars show the standard deviations of three independent measurements.

To further optimize the performance of DNase degradation-based CL detection, we investigated the effects of varying amounts of DNase I on the efficiency of release of CL labels from LSA-MPs by monitoring the changes in CL intensity. In the pre-experiment, 15 units of DNase I was employed to degrade DNA for different time periods (10–30 min) according to the manufacturer's instructions, but no obvious difference in CL intensity was observed (Figure S4, Supporting Information); thus, 10 min was chosen as a sufficient amount of time for DNA degradation. The CL intensity of the released CL labels was found to increase with increasing amounts of DNase I (2.5–10 units). With greater amounts of DNase I, the intensity stabilized (Figure 3A), indicating that 10 units was sufficient to degrade DNA. Moreover, the CL intensity of the remaining LSA-MPs was slightly higher than that of the negative control, possibly because DNase I could not access the DNA near the LSA-MP surface, resulting in a few retained CL labels on the LSA-MPs. Thus, 10 units of DNase I was chosen as an appropriate amount for DNA degradation in the following experiments.

Several other parameters, including the concentration of DNA-capture probes, hybridization temperature, and hybridization time, were investigated by monitoring the changes in CL intensity to establish the optimal conditions for HBV detection. As shown in Figure 3B, the CL intensity increased with increasing concentrations of aminated DNA-capture probes, reached a maximum at 5  $\mu\text{M}$ , and then decreased, possibly because of steric hindrance from excess probes. The CL intensity increased over the range of 40–50  $^{\circ}\text{C}$  and then decreased at higher probe hybridization temperatures (Figure 3C). Thus, the optimal hybridization temperature was 50  $^{\circ}\text{C}$ . The CL intensity increased between 1 and 30 min and then remained nearly constant (Figure 3D), probably because the LSA-MPs were saturated with the probes after 30 min. Consequently, a probe concentration of 5  $\mu\text{M}$ , a hybridization temperature of 50  $^{\circ}\text{C}$ , and a hybridization time of 30 min were selected as the optimal parameters for subsequent experiments.

The performance of CL detection on LSA-MPs was compared to that of the previously reported carboxylated MPs (CMPs).<sup>33–35</sup> The optimal conditions for CMP-based HBV detection were as follows: probe concentration of 2  $\mu\text{M}$ , hybridization temperature of 50  $^{\circ}\text{C}$ , and hybridization time of

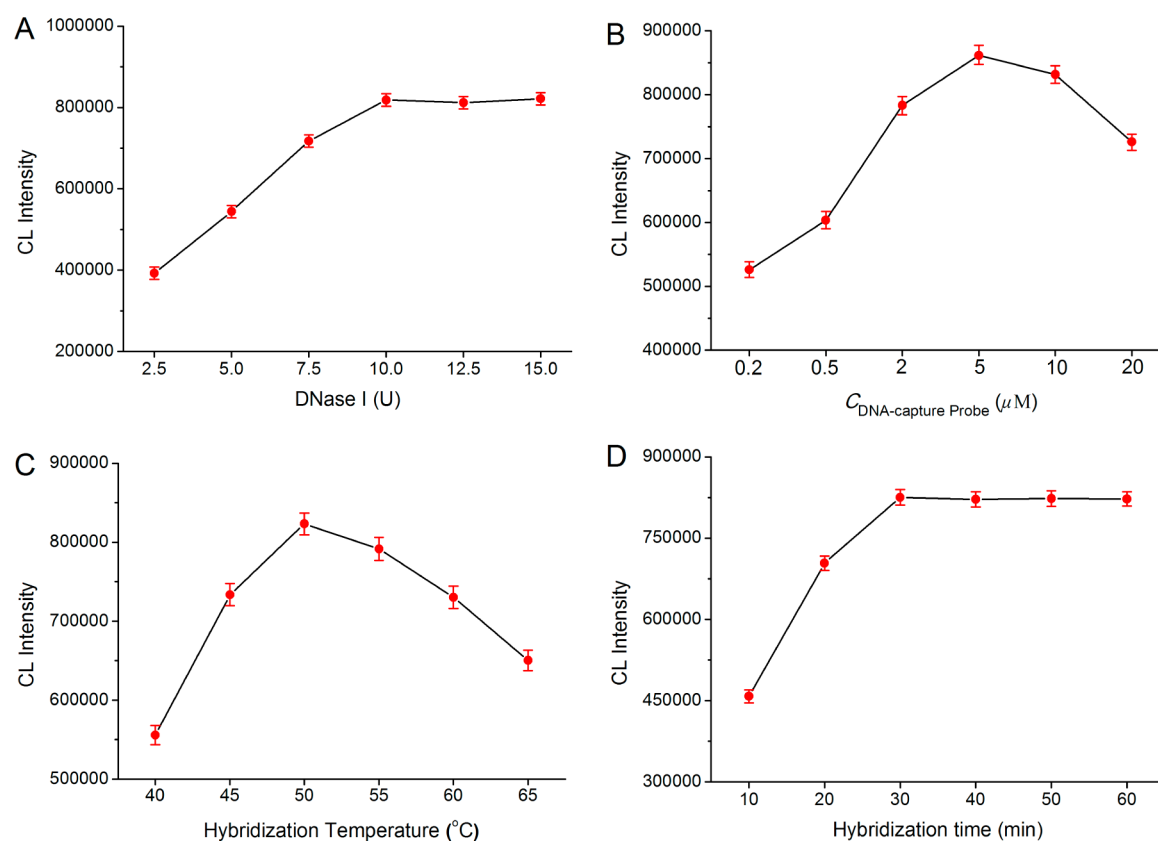


**Figure 3.** Optimizations of assay parameters. CL intensity vs the amount of DNase I (A), concentration of the DNA-capture probe (B), hybridization temperature (C), and hybridization time (D). Error bars show standard deviations of three independent measurements.

30 min (Figure S5, Supporting Information). As shown in Figure 4, the CL intensity was approximately 2-fold higher with

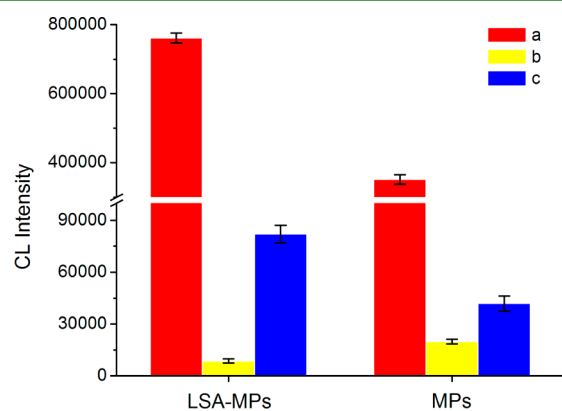


**Figure 4.** Comparison of HBV detection between LSA-MPs and MPs. CL detection of released CL labels (a), remaining MPs after releasing CL labels (b), and MPs retaining CL labels (c). Error bars show standard deviations of three independent measurements.

LSA-MPs when compared to that with CMPs, revealing a significant improvement in HBV detection. The higher CL intensity from released CL labels (a in Figure 4) coupled with the lower CL intensity of the remaining MPs (b in Figure 4) demonstrated the higher efficiency of release of CL labels from LSA-MPs compared to that from CMPs. CL detection assays of MPs retaining CL labels illustrated the more efficient hybridization on LSA-MPs compared to that on CMPs (c in Figure 4). These results indicated that the LSA-MPs can

provide CL-based detection of target pathogens in a manner remarkably superior to that of previously reported CL-based approaches.

The sensitivity of this detection approach under the optimized experimental conditions was assessed by monitoring CL intensities during the detection of the diluted HBV amplicon. CL intensities were plotted as a function of the log of various concentrations of HBV amplicons, and the results are shown in Figure 5. A calibration curve in the range of  $10^4$ – $10^8$  fM showed an approximately linear correlation between HBV amplicon concentration and CL intensity. At concentrations of  $<10^4$  or  $>10^8$  fM, the CL intensity leveled off and deviated from

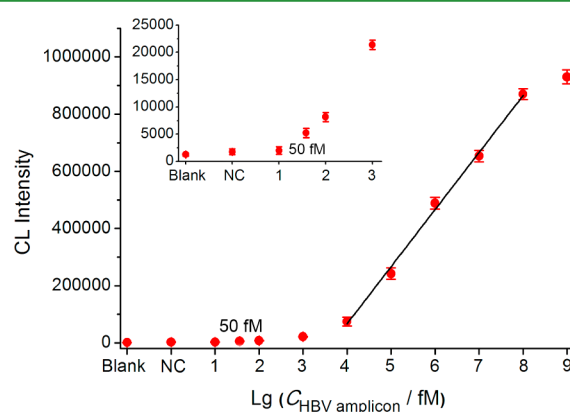


**Figure 5.** CL intensities plotted vs the log of various concentrations of HBV amplicons. Error bars show standard deviations of three independent measurements.

the calibration curve. The detection limit defined by a signal-to-noise ratio of 3 was determined to be 50 fM, which was superior to those of most previously reported CL methods (Table 1).<sup>39,43–54</sup> More importantly, this technique is ultrasensitive in the detection of target pathogens in clinical samples.

**Table 1. Comparison of Nucleic Acid Detection Sensitivities with Different CL Methods**

solid phase	label	CL system	DNA length (bp)	detection limit
MP	HRP	HRP/H <sub>2</sub> O <sub>2</sub> /luminol	20	0.1 pM <sup>39</sup>
MP	AP	AP/AMPPD	27	0.4 pM <sup>43</sup>
MP	AP	AP/AMPPD	31	3.6 pM <sup>44</sup>
MP	DNAzyme	H <sub>2</sub> O <sub>2</sub> /luminol	30	0.1 nM <sup>45</sup>
glass plate	DNAzyme	H <sub>2</sub> O <sub>2</sub> /luminol	36	1 nM <sup>46</sup>
MP	Au NP	Au <sup>3+</sup> /luminol	30	1 pM <sup>47</sup>
glass slide	Pt NP	Pt/H <sub>2</sub> O <sub>2</sub> /luminol	27	10 pM <sup>48</sup>
MP	HRP	HRP/H <sub>2</sub> O <sub>2</sub> /luminol	31	0.1 pM <sup>49</sup>
plate	irregular Au NP	Au/luminol/H <sub>2</sub> O <sub>2</sub>	33	13 pM <sup>50</sup>
polystyrene microwell	Au NP	H <sub>2</sub> O <sub>2</sub> /luminol/AuCl <sup>4+</sup>	30	0.1 pM <sup>51</sup>
polystyrene microwell	silver NP	Ag <sup>+</sup> /Mn <sub>2</sub> <sup>+</sup> /K <sub>2</sub> S <sub>2</sub> O <sub>8</sub> /H <sub>3</sub> PO <sub>4</sub> /luminol	30	5 fM <sup>52</sup>
MP	Au NP	Au <sup>3+</sup> /luminol	33	0.1 fM <sup>53</sup>
MP	AP	AP/AMPPD	277	5 pM <sup>54</sup>
LSA-MP (this study)	AP	AP/AMPPD	126	50 fM

Encouraged by the excellent selectivity and sensitivity in the detection of HBV, we employed sera of 15 patients with hepatitis B and sera from five healthy subjects to evaluate the capability and reproducibility of the developed technique. As illustrated in Figure 6, HBV was detected in the sera of all 15

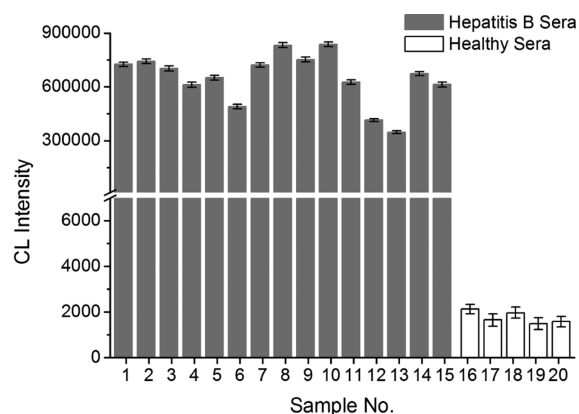


**Figure 6.** HBV detection in human sera using the enhanced CL detection technique based on CL labels released from LSA-MPs. Error bars show standard deviations of three independent measurements.

patients; the CL intensities were huge and significantly higher than those of the negative controls (see Figures 1B and 5). Meanwhile, the signals for the five healthy samples were tiny and similar to the values of the negative controls (see Figures 1B and 5). These results indicate that this technique offers unambiguous accuracy and repeatability in the detection of HBV. Furthermore, this technique can be used for the identification of ultralow concentrations of target pathogens

in clinical samples with high selectivity and excellent reproducibility.

## CONCLUSIONS

In summary, we have developed a novel, enhanced detection technique based on CL labels released from LSA-MPs for the clinical detection of target pathogens. To the best of our knowledge, this is the first attempt to explore the separation of targets from MPs for enhanced CL detection, in an effort to overcome attenuated CL signals caused by the inner filter-like effect observed with MPs. Moreover, the introduction of LSA contributed to the prominent improvement in CL detection as compared with the use of conventional MPs. In contrast to LSA ultrasonication, the DNase degradation strategy was shown to be simple and highly efficient for enhanced CL detection. The release of CL labels significantly improved the MP-based CL detection assay. Because of its ultrasensitivity and wide detection range, this novel technique facilitated the detection of very low levels of target pathogens from clinical samples and simultaneously demonstrated high selectivity and excellent reproducibility. Although only HBV was detected as a proof of concept, this approach could be readily applicable to the detection of other infectious pathogens, such as HCV, HIV, and TP.

## ASSOCIATED CONTENT

### Supporting Information

Additional figures and tables. This material is available free of charge via the Internet at <http://pubs.acs.org>.

## AUTHOR INFORMATION

### Corresponding Authors

\*E-mail: [nyhe1958@163.com](mailto:nyhe1958@163.com). Phone and fax: 86-25-83790885.

\*E-mail: [lizhiyangcn@qq.com](mailto:lizhiyangcn@qq.com).

### Author Contributions

H.Y. and W.L. contributed equally to this work.

### Notes

The authors declare no competing financial interest.

## ACKNOWLEDGMENTS

This work was supported by the National Key Program for Developing Basic Research (2014CB744501 and 2010CB933903), the 863 Program (2012AA022703), the National Key Special Science Program (2013ZX10004103-002), the National Natural Science Foundation of China (61201033, 61471168, and 61271056), the Eleventh Foundation for Jiangsu Provincial Science and Technology Innovation & Transformation of Health Science and Technology Achievements of 2012 (BL2012067), the Clinical Science and Technology Special Projects in Jiangsu Province (BL2014094), and A Project Funded by the Priority Academic Program Development of Jiangsu Higher Education Institutions (PAPD).

## REFERENCES

- (1) Lovén, J.; Orlando, D. A.; Sigova, A. A.; Lin, C. Y.; Rahl, P. B.; Burge, C. B.; Levens, D. L.; Lee, T. I.; Young, R. A. Revisiting Global Gene Expression Analysis. *Cell* **2012**, *151*, 476–482.
- (2) Wang, X.; Spandidos, A.; Wang, H.; Seed, B. PrimerBank: A PCR Primer Database for Quantitative Gene Expression Analysis, 2012 update. *Nucleic Acids Res.* **2012**, *40*, D1144–D1149.
- (3) Whibley, C.; Pharoah, P. D. P.; Hollstein, M. P53 Polymorphisms: Cancer Implications. *Nat. Rev. Cancer* **2009**, *9*, 95–107.

- (4) Wang, W.; Zhao, Y.; Jin, Y. Gold-Nanorod-Based Colorimetric and Fluorescent Approach for Sensitive and Specific Assay of Disease-Related Gene and Mutation. *ACS Appl. Mater. Interfaces* **2013**, *5*, 11741–11746.
- (5) Schneider, G. F.; Dekker, C. DNA Sequencing with Nanopores. *Nat. Biotechnol.* **2012**, *30*, 326–328.
- (6) Mardis, E. R. A Decade's Perspective on DNA Sequencing Technology. *Nature* **2011**, *470*, 198–203.
- (7) Harper, J. C.; SenGupta, S. B. Preimplantation Genetic Diagnosis: State of the Art 2011. *Hum. Genet.* **2012**, *131*, 175–186.
- (8) Fauci, A. S.; Morens, D. M. The Perpetual Challenge of Infectious Diseases. *N. Engl. J. Med.* **2012**, *366*, 454–461.
- (9) Lou, X.; Zhang, Y. Mechanism Studies on NanoPCR and Applications of Gold Nanoparticles in Genetic Analysis. *ACS Appl. Mater. Interfaces* **2013**, *5*, 6276–6284.
- (10) Yang, T.; Meng, L.; Wang, X.; Wang, L.; Jiao, K. Direct Electrochemical DNA Detection Originated from the Self-Redox Signal of Sulfonated Polyaniline Enhanced by Graphene Oxide in Neutral Solution. *ACS Appl. Mater. Interfaces* **2013**, *5*, 10889–10894.
- (11) Gao, C.; Guo, Z.; Liu, J.; Huang, X. The New Age of Carbon Nanotubes: An Updated Review of Functionalized Carbon Nanotubes in Electrochemical Sensors. *Nanoscale* **2012**, *4*, 1948–1963.
- (12) Kim, J. H.; Kataoka, M.; Jung, Y. C.; Ko, Y. I.; Fujisawa, K.; Hayashi, T.; Kim, Y. A.; Endo, M. Mechanically Tough, Electrically Conductive Polyethylene Oxide Nanofiber Web Incorporating DNA-Wrapped Double-Walled Carbon Nanotubes. *ACS Appl. Mater. Interfaces* **2013**, *5*, 4150–4154.
- (13) Gao, A.; Lu, N.; Wang, Y.; Dai, P.; Li, T.; Gao, X.; Wang, Y.; Fan, C. Enhanced Sensing of Nucleic Acids with Silicon Nanowire Field Effect Transistor Biosensors. *Nano Lett.* **2012**, *12*, 5262–5268.
- (14) Homola, J. Surface Plasmon Resonance Sensors for Detection of Chemical and Biological Species. *Chem. Rev.* **2008**, *108*, 462–493.
- (15) Barhoumi, A.; Zhang, D.; Tam, F.; Halas, N. J. Surface-Enhanced Raman Spectroscopy of DNA. *J. Am. Chem. Soc.* **2008**, *130*, 5523–5529.
- (16) Müller, D. J.; Duffr en, Y. F. Atomic Force Microscopy as a Multifunctional Molecular Toolbox in Nanobiotechnology. *Nat. Nanotechnol.* **2008**, *3*, 261–269.
- (17) Minunni, M.; Tombelli, S.; Fonti, J.; Spiriti, M. M.; Mascini, M.; Bogani, P.; Buiatti, M. Detection of Fragmented Genomic DNA by PCR-Free Piezoelectric Sensing Using a Denaturation Approach. *J. Am. Chem. Soc.* **2005**, *127*, 7966–7967.
- (18) Wang, G.; Zhang, R.; Xu, C.; Zhou, R.; Dong, J.; Bai, H.; Zhan, X. Fluorescence Detection of DNA Hybridization Based on the Aggregation-Induced Emission of a Perylene-Functionalized Polymer. *ACS Appl. Mater. Interfaces* **2014**, *6*, 11136–11141.
- (19) Su, S.; Fan, J.; Xue, B.; Yuwen, L.; Liu, X.; Pan, D.; Fan, C.; Wang, L. DNA-Conjugated Quantum Dot Nanoprobe for High-Sensitivity Fluorescent Detection of DNA and micro-RNA. *ACS Appl. Mater. Interfaces* **2014**, *6*, 1152–1157.
- (20) Zhao, L.; Sun, L.; Chu, X. Chemiluminescence Immunoassay. *TrAC, Trends Anal. Chem.* **2009**, *28*, 404–415.
- (21) Bronstein, I.; Mcgrath, P. Chemiluminescence Lights Up. *Nature* **1989**, *338*, 599–600.
- (22) Han, M. S.; Lytton-Jean, A. K. R.; Oh, B. K.; Heo, J.; Mirkin, C. A. Colorimetric Screening of DNA-Binding Molecules with Gold Nanoparticle Probes. *Angew. Chem., Int. Ed.* **2006**, *45*, 1807–1810.
- (23) Lin, Y. Z.; Chang, P. L. Colorimetric Determination of DNA Methylation Based on the Strength of the Hydrophobic Interactions between DNA and Gold Nanoparticles. *ACS Appl. Mater. Interfaces* **2013**, *5*, 12045–12051.
- (24) Baeissa, A.; Dave, N.; Smith, B. D.; Liu, J. DNA-Functionalized Monolithic Hydrogels and Gold Nanoparticles for Colorimetric DNA Detection. *ACS Appl. Mater. Interfaces* **2010**, *2*, 3594–3600.
- (25) Garc a-Campa a, A. M.; Lara, F. J.; G miz-Gracia, L.; Huertas-P rez, J. F. Chemiluminescence Detection Coupled to Capillary Electrophoresis. *TrAC, Trends Anal. Chem.* **2009**, *28*, 973–986.
- (26) Geissler, M.; Roy, E.; Diaz-Quijada, G. A.; Galas, J. C.; Veres, T. Microfluidic Patterning of Miniaturized DNA Arrays on Plastic Substrates. *ACS Appl. Mater. Interfaces* **2009**, *1*, 1387–1395.
- (27) Iranifam, M. Analytical Applications of Chemiluminescence-Detection Systems Assisted by Magnetic Microparticles and Nanoparticles. *TrAC, Trends Anal. Chem.* **2013**, *51*, S1–70.
- (28) He, N.; Wang, F.; Ma, C.; Li, C.; Zeng, X.; Deng, Y.; Zhang, L.; Li, Z. Chemiluminescence Analysis for HBV-DNA Hybridization Detection with Magnetic Nanoparticles Based DNA Extraction from Positive Whole Blood Samples. *J. Biomed. Nanotechnol.* **2013**, *9*, 267–273.
- (29) Oliveira, O. N., Jr.; Iost, R. M.; Siqueira, J. R., Jr.; Crespilho, F. N.; Caseli, L. Nanomaterials for Diagnosis: Challenges and Applications in Smart Devices Based on Molecular Recognition. *ACS Appl. Mater. Interfaces* **2014**, *6*, 14745–14766.
- (30) Parolo, C.; Merko ci, A. Paper-Based Nanobiosensors for Diagnostics. *Chem. Soc. Rev.* **2013**, *42*, 450–457.
- (31) Rosi, N. L.; Mirkin, C. A. Nanostructures in Biodiagnostics. *Chem. Rev.* **2005**, *105*, 1547–1562.
- (32) Wang, H.; Yang, R.; Yang, L.; Tan, W. Nucleic Acid Conjugated Nanomaterials for Enhanced Molecular Recognition. *ACS Nano* **2009**, *3*, 2451–2460.
- (33) Li, Z.; He, L.; He, N.; Deng, Y.; Shi, Z.; Wang, H.; Li, S.; Liu, H.; Wang, Z.; Wang, D. Polymerase Chain Reaction Coupling with Magnetic Nanoparticles-Based Biotin-Avidin System for Amplification of Chemiluminescent Detection Signals of Nucleic Acid. *J. Nanosci. Nanotechnol.* **2011**, *11*, 1074–1078.
- (34) Wang, F.; Ma, C.; Zeng, X.; Li, C.; Deng, Y.; He, N. Chemiluminescence Molecular Detection of Sequence-Specific HBV-DNA Using Magnetic Nanoparticles. *J. Biomed. Nanotechnol.* **2012**, *8*, 786–790.
- (35) Tang, Y.; Zou, J.; Ma, C.; Ali, Z.; Li, Z.; Li, X.; Ma, N.; Mou, X.; Deng, Y.; Zhang, L.; Li, K.; Lu, G.; Yang, H.; He, N. Highly Sensitive and Rapid Detection of *Pseudomonas aeruginosa* Based On Magnetic Enrichment and Magnetic Separation. *Theranostics* **2013**, *3*, 85–92.
- (36) Yang, H.; Liang, W.; Si, J.; Li, Z.; He, N. Long Spacer Arm-Functionalized Magnetic Nanoparticle Platform for Enhanced Chemiluminescent Detection of Hepatitis B Virus. *J. Biomed. Nanotechnol.* **2014**, *10*, 3610–3619.
- (37) Fuentes, M.; Mateo, C.; Rodriguez, A.; Casqueiro, M.; Tercero, J. C.; Riese, H. H.; Fernandez-Lafuente, R.; Guisan, J. M. Detecting Minimal Traces of DNA Using DNA Covalently Attached to Superparamagnetic Nanoparticles and Direct PCR-ELISA. *Biosens. Bioelectron.* **2006**, *21*, 1574–1580.
- (38) Li, Z.; Yang, H.; He, N.; Liang, W.; Ma, C.; Shah, M. A.; Tang, Y.; Li, S.; Liu, H.; Jiang, H.; Guo, Y. Solid-phase Hybridization Efficiency Improvement on the Magnetic Nanoparticle Surface by Using Dextran as Molecular Arms. *J. Biomed. Nanotechnol.* **2013**, *9*, 1945–1949.
- (39) Cai, S.; Lau, C.; Lu, J. Sequence-Specific Detection of Short-Length DNA via Template-Dependent Surface-Hybridization Events. *Anal. Chem.* **2010**, *82*, 7178–7184.
- (40) Jung, Y. K.; Kim, T. W.; Jung, C.; Cho, D. Y.; Park, H. G. A Polydiacetylene Microchip Based on a Biotin-Streptavidin Interaction for the Diagnosis of Pathogen Infections. *Small* **2008**, *4*, 1778–1784.
- (41) Suck, D.; Oefner, C. Structure of DNase I at 2.0   Resolution Suggests a Mechanism for Binding to and Cutting DNA. *Nature* **1986**, *321*, 620–625.
- (42) Koda, S.; Taguchi, K.; Futamura, K. Effects of Frequency and a Radical Scavenger on Ultrasonic Degradation of Water-Soluble Polymers. *Ultrason. Sonochem.* **2011**, *18*, 276–281.
- (43) He, L.; Li, Z.; Fu, J.; Wang, F.; Ma, C.; Deng, Y.; Shi, Z.; Wang, H.; He, N. Preparation of SiO<sub>2</sub>/(PMMA/Fe<sub>3</sub>O<sub>4</sub>) Nanoparticles Using Linolenic Acid as Crosslink Agent for Nucleic Acid Detection Using Chemiluminescent Method. *J. Nanosci. Nanotechnol.* **2011**, *11*, 2256–2262.
- (44) Li, Z.; Li, W.; Cheng, Y.; Hao, L. Chemiluminescent Detection of DNA Hybridization and Single-Nucleotide Polymorphisms on a

Solid Surface Using Target-Primed Rolling Circle Amplification. *Analyst* **2008**, *133*, 1164–1168.

(45) Cao, Z.; Li, Z.; Zhao, Y.; Song, Y.; Lu, J. Magnetic Bead-Based Chemiluminescence Detection of Sequence-Specific DNA by Using Catalytic Nucleic Acid Labels. *Anal. Chim. Acta* **2006**, *557*, 152–158.

(46) Pavlov, V.; Xiao, Y.; Gill, R.; Dishon, A.; Kotler, M.; Willner, I. Amplified Chemiluminescence Surface Detection of DNA and Telomerase Activity Using Catalytic Nucleic Acid Labels. *Anal. Chem.* **2004**, *76*, 2152–2156.

(47) Fan, A.; Lau, C.; Lu, J. Colloidal Gold-Polystyrene Bead Hybrid for Chemiluminescent Detection of Sequence-Specific DNA. *Analyst* **2008**, *133*, 219–225.

(48) Gill, R.; Polsky, R.; Willner, I. Pt Nanoparticles Functionalized with Nucleic Acid Act as Catalytic Labels for the Chemiluminescent Detection of DNA and Proteins. *Small* **2006**, *2*, 1037–1041.

(49) Li, H.; He, Z. Magnetic bead-based DNA Hybridization Assay with Chemiluminescence and Chemiluminescent Imaging Detection. *Analyst* **2009**, *134*, 800–804.

(50) Wang, Z.; Hu, J.; Jin, Y.; Yao, X.; Li, J. In Situ Amplified Chemiluminescent Detection of DNA and Immunoassay of IgG Using Special-Shaped Gold Nanoparticles as Label. *Clin. Chem.* **2006**, *52*, 1958–1961.

(51) Li, Z.; Liu, C.; Fan, Y.; Wang, Y.; Duan, X. Chemiluminescent Detection of DNA Hybridization Using Gold Nanoparticles as Labels. *Anal. Bioanal. Chem.* **2007**, *387*, 613–618.

(52) Liu, C.; Li, Z.; Du, B.; Duan, X.; Wang, Y. Silver Nanoparticle-Based Ultrasensitive Chemiluminescent Detection of DNA Hybridization and Single-Nucleotide Polymorphisms. *Anal. Chem.* **2006**, *78*, 3738–3744.

(53) Li, X.; Li, W.; Zhang, S. Chemiluminescence DNA Biosensor Based on Dual-Amplification of Thrombin and Thiocyanuric Acid-Gold Nanoparticle Network. *Analyst* **2010**, *135*, 332–336.

(54) Yang, H.; Guo, Y.; Li, S.; Lan, G.; Jiang, Q.; Yang, X.; Fan, J.; Ali, Z.; Tang, Y.; Mou, X.; Liu, H.; Shah, M. A.; Jin, S.; Jiang, H.; Li, Z. Magnetic Bead-Based Chemiluminescent Assay for Ultrasensitive Detection of Pseudorabies Virus. *J. Nanosci. Nanotechnol.* **2014**, *14*, 3337–3342.